Petroleum and Coal

Article **Open Access**

Numerical Modeling of Simultaneous Distributions of Velocity, Pressure and Temperature in Waxy Crude Oil Flow Using Computational Fluid Dynamics Technique

Amirabbas Mohammadi, Ntandoyenkosi Malusi Mkhize, Amir H. Mohammadi *

Discipline of Chemical Engineering, School of Engineering, University of KwaZulu-Natal, Howard College Campus, King George V Avenue, Durban 4041, South Africa

Received November 23, 2022; Accepted May 26, 2023

Abstract

To compensate for the decrease of velocity and pressure of waxy crude oil flow in a pipeline under the conditions that it exhibits non-Newtonian behavior, engineers would have to optimize the transmission power. This objective requires correct modeling of the rheological behavior and estimating the distributions of velocity, pressure, and temperature in the fluid along the pipeline. The rheological behavior of crude oil is highly dependent on wax content, shear rate, and temperature. In this work, to study the influence of wax content, two types of crude oils with different paraffin contents, referred to as reference crude oils, were studied. The results of shear-rotary tests using an Anton Paar MCR 302 indicate that in a specific range of shear rates, the reference crude oils are non-Newtonian at the studied temperatures of pipe wall and inlet. Considering the Power-law model for describing the rheological behaviors of these fluids, two dimensionless numerical models are proposed. Using Computational Fluid Dynamics (CFD) technique, the velocity, pressure, and temperature of each reference crude oil were modeled. The accuracy of the model and input data were successfully evaluated against results reported in the literature.

Keywords: *Waxy crude oil; Non-Newtonian fluid; Power-law model; Dimensionless; Computational Fluid Dynamics (CFD).*

1. Introduction

In modern transmission processes delivering crude oils from reservoirs to refineries and between processing units, because of temperature decrease and heat transfer between the fluid and pipeline wall and increase in paraffin content, the fluid may exhibit non-Newtonian behavior [1-9]. In these cases, engineers and processing equipment designers to compensate for the decrease in the velocity and pressure of the flow need to increase the transmission power including the power of pumps, transmission networks, and heat exchangers. To this end, the rheological behavior of the crude oil flowing the pipeline must be described. Afterward, it is necessary to estimate the velocity and pressure of the fluid flow in different sections of the pipeline based on fluid behavior.

The study of flow variables including velocity, pressure, and temperature based on a correct description of fluid rheological behavior has received considerable attention from many researchers in this field. Many of these researchers have used the structural equation of Power-law in describing fluid rheological behavior [10-12]. In these studies, in addition to the geometrical variation of flow paths (channel, pipe and parallel plates), several different boundary conditions and environmental or laboratory conditions are observed. These studies take into account mass and heat transfer phenomena separately and ignore viscous dissipation; also the calculation of velocity, pressure, and temperature are not simultaneously carried out.

Some researchers have studied heat transfer in fully developed flow [13] of Power-law fluids ignoring the heat dissipation [14] and the viscosity variation caused by temperature changes, to provide a relation for the maximum dimensionless velocity on the centerline. By ignoring

heat dissipation, some researchers have studied the heat transfer in fully developed flow of a Power-law fluid in a pipe [15]. The relation proposed for the linear distribution of shear stress on the pipe cross-section indicates a zero shear stress on the pipe centerline, and a no-slip condition on the pipe wall has been considered. Furthermore, the rheological behavior and heat transfer of a Power-law fluid between parallel plates was studied. In this regard, by using the relationship between the Fanning friction factor [16] and Reynolds number [17-18], the fully developed flow of Power-law fluid between two parallel plates has been studied in a certain range of flow behavior index (n=1 and n=0.5) to estimate the pressure drop of the flow of a Power-law fluid [19].

The numerical model presented in this study is based on the rheology of paraffinic crude oil and is developed considering the dependence of mass transfer and heat transfer and also viscous dissipation in the fluid. The rheological behavior of crude oil is highly dependent on paraffin content, shear rate, and temperature. To study the influence of paraffin content, two types of paraffinic crude oil with different paraffin contents (Table 1), referred to as reference crude oils are studied.

Table 1. Physicochemical properties of reference crude oils [20]

Reference crude oils	A	B
Density @ 26°C (g/cm^3)	0.872	0.896
API Gravity	38.50	22.30
Paraffin content (wt.%)	7	25
Sulfur Content (wt.%)	0.41	4.25
Water content (vol.%)	<0.025	<0.05
Pour point (°C)	12	10
Nitrogen content (wt.%)	0.08	0.12

In this study, the temperatures of the pipe wall and inlet are 22 and 26°C, respectively. According to the specifications of the reference crude oils, the difference between the pour points and the desired temperatures completely supports the assumption of no appearance of a solid phase at 22 and 26°C. Furthermore, the shear stresses exerted on the reference crude oil flow are in the shear rate range of 100-600 s^{-1}. Under these conditions, the results of digital rheometric tests using an Anton Paar MCR 302 including the experimental data of the viscosity-shear rate curves (Table 2) and non-linear flow curves (shear stress-strain rate curves) [20], indicate that the reference crude oils are non-Newtonian. Besides, for the flow curve approximation and the experimental data matching, the Power-law has been used for each of the reference crude oils. Accordingly, by fitting the Power-law model to experimental data from flow curves, the model indices (the consistency index and the flow behavior index) have been obtained for both reference crude oils at the two temperatures (Table 3) [20]. Moreover, the thermophysical properties of the reference crude oils, consisting of thermal conductivity and specific heat capacity, experimentally have been measured (Table 4) [21].

Table 2. Experimental viscosity (Pa.s)-shear rate (s^{-1}) curves data for reference crude oils at 22 and 26°C [21]

	26°C		22°C	
Shear rate (s^{-1})	A	B	A	B
100	0.091	0.410	0.098	0.525
120	0.091	0.343	0.098	0.462
140	0.091	0.292	0.098	0.401
170	0.091	0.257	0.098	0.342
200	0.091	0.228	0.098	0.291
250	0.091	0.202	0.098	0.246
300	0.091	0.182	0.098	0.201
380	0.091	0.160	0.098	0.168
450	0.091	0.141	0.098	0.149
600	0.091	0.123	0.098	0.127

Table 3. Power-law equations for reference crude oils at 22 and 26°C [20]

Temperature (°C)	Reference crude oil	Power-law equation
26	A	$\tau = 0.0042(\dot{\gamma})^{0.9953}$
	B	$\tau = 6.012(\dot{\gamma})^{0.5109}$
22	A	$\tau = 0.0067(\dot{\gamma})^{0.9902}$
	B	$\tau = 8.9012(\dot{\gamma})^{0.5003}$

2. Governing equations

It is assumed that the flow of Power-law crude oil enters a horizontal pipe with length ℓ, diameter $2R$ and wall temperature T_w at uniform velocity v_{in}, pressure P_{in}, and temperature T_{in} ($T_w < T_{in}$) (Figure 1). Moreover, viscosity, thermal conductivity and specific heat capacity of the fluid respectively are μ, K and c_P along the pipe at temperature T. The flow is simultaneously developing from the standpoint of fluid dynamics. Put differently, the velocity and temperature gradients are changing along the pipe.

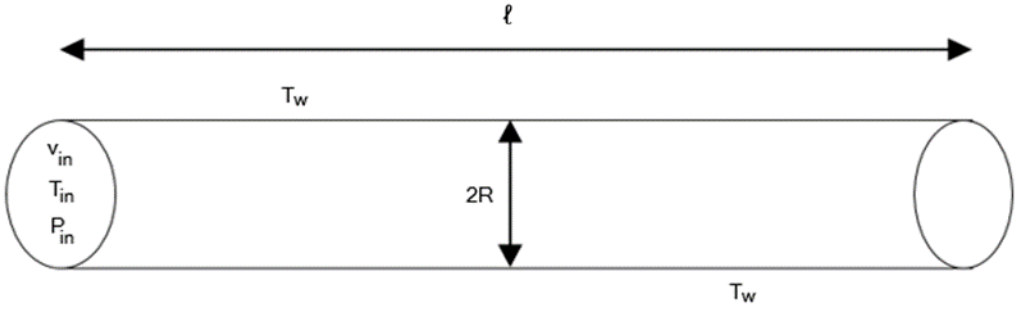

Figure 1 Horizontal pipe with wall temperature T_w in which reference crude oil flows

Since the pipe wall temperature and the temperature of Power-law crude oil at the pipe inlet are, respectively, 22 and 26°C, so based on the estimated range for flow behavior index [20] the Reynolds number has been calculated for each reference crude oil using both Ryan's and Mishra's equations [17-18].

Considering the range defined for laminar flow [17-18], a laminar flow is expected for each of the reference crude oils in the pipe. Accordingly, the fluid density can be assumed to remain fixed and considering a mass balance and a momentum balance, the problem is governed by Navier–Stokes equations including continuity and momentum equations, in addition to the energy equation, as follows:

$$\frac{\partial u}{\partial x} + \frac{\partial v}{\partial y} = 0 \quad (1)$$

$$\rho\left(\frac{\partial u}{\partial t} + \frac{\partial u^2}{\partial x} + \frac{\partial uv}{\partial y}\right) = \rho g_x - \frac{\partial P}{\partial x} + \mu\left(\frac{\partial^2 u}{\partial x^2} + \frac{\partial^2 v}{\partial y^2}\right) \quad (2)$$

$$\rho\left(\frac{\partial v}{\partial t} + \frac{\partial v^2}{\partial y} + \frac{\partial vu}{\partial x}\right) = \rho g_y - \frac{\partial P}{\partial y} + \mu\left(\frac{\partial^2 u}{\partial x^2} + \frac{\partial^2 v}{\partial y^2}\right) \quad (3)$$

$$\frac{\partial T}{\partial t} + \frac{\partial (uT)}{\partial x} + \frac{\partial (vT)}{\partial y} = \frac{K}{\rho c_P}\left(\frac{\partial^2 T}{\partial x^2} + \frac{\partial^2 T}{\partial y^2}\right) - \mu\left(2\left(\frac{\partial u}{\partial x}\right)^2 + 2\left(\frac{\partial v}{\partial y}\right)^2 + \left(\frac{\partial u}{\partial y} + \frac{\partial v}{\partial x}\right)^2\right) \quad (4)$$

In the equations above, u is the fluid velocity in the x direction and v is the fluid velocity in the y direction. The parameters of velocity, pressure and temperature are unknowns, whereas the input data (known parameters) include density, viscosity, thermal conductivity and specific heat capacity of the fluid. Moreover, the computational domain is set in $0 \leq x \leq \ell$ and $0 \leq y \leq 2R$.

3. Initial and boundary conditions

Under the ambient temperature condition, the pipe wall temperature is below that of the fluid especially below its temperature at the inlet ($T_{in} > T_w$). On the one hand, as a result of the heat transfer from the fluid to the pipe walls, the temperature of the fluid adjacent to the inner surface of the pipe remains close to that of the wall. Considering the increased viscosity of the fluid near the internal surface of the pipe, the no-slip assumption applies and the velocity of the fluid can be assumed to be negligible over the pipe walls (Figure 2).

$$\begin{cases} x = 0 & \begin{cases} u = v_{in} \\ v = 0 \end{cases}, \quad P = P_{in} \quad and \quad T = T_{in} \\ \begin{cases} y = 0 \\ y = 2R \end{cases} & u_{slip} = 0 \quad and \quad v_{slip} = 0 \end{cases} \tag{5}$$

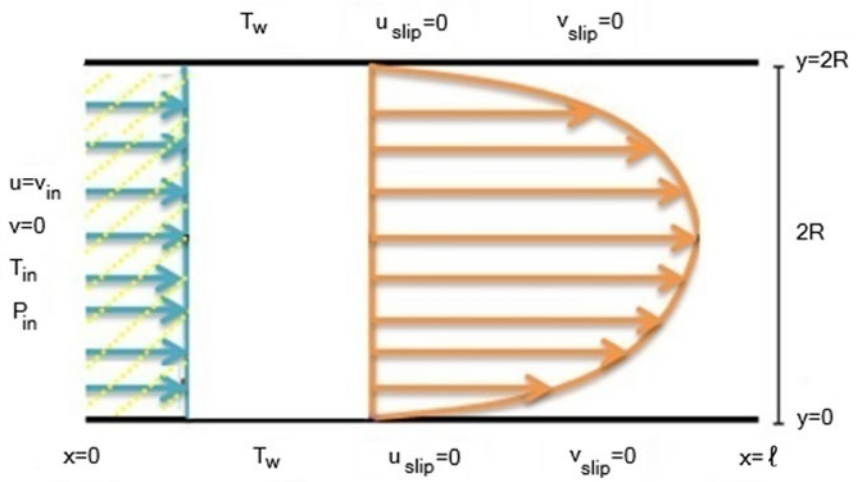

Figure 2. Velocity, temperature, and pressure of fluid at pipe inlet / velocity and temperature of fluid over inner surface of pipe

4. Dimensionless governing equations

The dimensionless form of the governing equations is obtained by introducing the dimensionless quantities and numbers. For the present study, Reynolds, Prandtl and Brinkman numbers are defined by the following relations, respectively:

$$Re = \frac{\rho.(v_{in})^{2-n}.(2R)^n}{\mu} \tag{6}$$

$$Pr = \frac{\mu.c_P.(v_{in})^{n-1}}{K(2R)^{n-1}} \tag{7}$$

$$Br = \frac{\mu.(v_{in})^{n-1}}{(2R)^{n-1}(T_w - T)K} \tag{8}$$

Considering $T > T_w$, Br is negative in the case where the fluid running through the pipe is cooling down. Also, the dimensionless quantities below are used to write the dimensionless forms of the governing equations.

$$x^* = \frac{x}{\ell} \tag{9}$$

$$y^* = \frac{y}{2R} \tag{10}$$

$$t^* = \frac{t.v_{in}}{\ell} \tag{11}$$

$$u^* = \frac{u}{v_{in}} \tag{12}$$

$$v^* = \frac{v}{v_{in}} \tag{13}$$

$$P^* = \frac{P}{P_{in}} \tag{14}$$

$$C_P^* = \frac{C_P}{C_{P_{in}}} \tag{15}$$

$$\rho^* = \frac{\rho}{\rho_{in}} \tag{16}$$

$$\mu^* = \frac{\mu}{\mu_{in}} \tag{17}$$

$$K^* = \frac{K}{K_{in}} \tag{18}$$

$$\theta = \frac{T - T_w}{T_{in} - T_w} \tag{19}$$

Based on the relations above:

$$\frac{\partial u^*}{\partial x^*}+\frac{\partial v^*}{\partial y^*}=0 \quad (20)$$

$$\frac{\partial u^*}{\partial t^*}+\frac{\partial u^{*2}}{\partial x^*}+\frac{\partial (u^*.v^*)}{\partial y^*}=\frac{\mu^*}{Re\left(\frac{\partial}{\partial x^*}\left(\frac{\partial u^*}{\partial x^*}\right)+\frac{\partial}{\partial y^*}\left(\frac{\partial v^*}{\partial y^*}\right)\right)\frac{\partial P^*}{\partial x^*}} \quad (21)$$

$$\frac{\partial v^*}{\partial t^*}+\frac{\partial v^{*2}}{\partial y^*}+\frac{\partial (v^*.u^*)}{\partial x^*}=\frac{\mu^*}{Re\left(\frac{\partial}{\partial y^*}\left(\frac{\partial v^*}{\partial y^*}\right)+\frac{\partial}{\partial x^*}\left(\frac{\partial u^*}{\partial x^*}\right)\right)\frac{\partial P^*}{\partial y^*}} \quad (22)$$

$$\frac{\partial \theta}{\partial t^*}+\frac{\partial (u^*.\theta)}{\partial x^*}+\frac{\partial (v^*.\theta)}{\partial y^*}=\frac{1}{Re.Pr\frac{K^*}{c_P^*}\left(\left(\frac{\partial \theta}{\partial x^*}\right)^2+\left(\frac{\partial \theta}{\partial y^*}\right)^2\right)}-\frac{Br}{Re.Pr\frac{\mu^*}{c_P^*}\left(2\left(\left(\frac{\partial u^*}{\partial x^*}\right)^2+\left(\frac{\partial v^*}{\partial y^*}\right)^2\right)+\left(\frac{\partial u^*}{\partial y^*}+\frac{\partial v^*}{\partial x^*}\right)^2\right)} \quad (23)$$

According to Eqs. (20) through (23), one must note that the viscous dissipation term appears only in the last term on the right side of the dimensionless energy equation and has no impact on dimensionless continuity and momentum equations. Further, according to Eq. (23), the dimensionless temperature gradient depends on the dimensionless velocity gradient of the fluid.

5. Modified governing dimensionless equations

Given that the flow behavior index, viscosity, thermal conductivity, and specific heat capacity of reference crude oils are functions of temperature, in cases where the difference between input and output temperatures is considerable, the above parameters are required to be calculated at each point of the computational domain separately, which is too complicated and even impossible. The fluid temperature along with its velocity and pressure are the unknowns in the computational domain and must be determined. If the temperature of the fluid is known all across the computational domain, then the fewer unknowns will remain at hand, and the parameters above can be calculated at any point in the computational domain (although with some difficulty).

Table 4. Thermal conductivity and specific heat capacity measured at temperatures 22 and 26°C for reference crude oils [21]

Reference crude oil	Temperature(°C)	Thermal conductivity (J/g °C)	Specific heat capacity (W/m °C)
A	26	1.831	0.138
	22	1.829	0.139
B	26	1.901	0.144
	22	1.898	0.145

The flow behavior indices in Table 3 are considered to be precise to two decimal places. In this case, when the temperature decreases from 26 to 22 °C, the flow behavior index doesn't change significantly for each of the reference crude oils A and B and respectively remains at 0.99 and 0.50. In these cases, the following results are obtained:

- The viscosity of reference crude oil A in the range of 100-600 s^{-1} can be considered 0.09 Pa.s.
- The viscosity of reference crude oil B is increased as the temperature decreases from 26 to 22 °C, but at both temperatures, the viscosity of the fluid is reduced as the shear rate rises. The viscosity of reference crude oil B can be considered 0.20 Pa.s with the mentioned precision.
- By the given precision, thermal conductivity and specific heat capacity measured for the reference crude oils A and B (Table 4), do not change with temperature variations, and respectively remain for the reference crude oil A at 1.83 J/g °C and 0.13 W/m °C, and for the reference crude oil B at 1.90 J/g °C and 0.14 W/m °C.

By taking into account the assumptions above for viscosity, thermal conductivity and specific heat capacity for each reference crude oil in Eqs. (15), (17) and (18), the governing dimensionless equations Eqs. (20) through (23) are modified into Eqs. (24) through (27).

$$\frac{\partial u^*}{\partial x^*}+\frac{\partial v^*}{\partial y^*}=0 \quad (24)$$

$$\frac{\partial u^*}{\partial t^*}+\frac{\partial u^{*2}}{\partial x^*}+\frac{\partial (u^*.v^*)}{\partial y^*}=\frac{1}{Re\left(\frac{\partial}{\partial x^*}\left(\frac{\partial u^*}{\partial x^*}\right)+\frac{\partial}{\partial y^*}\left(\frac{\partial v^*}{\partial y^*}\right)\right)\frac{\partial P^*}{\partial x^*}} \quad (25)$$

$$\frac{\partial v^*}{\partial t^*}+\frac{\partial {v^*}^2}{\partial y^*}+\frac{\partial (v^*.u^*)}{\partial x^*}=\frac{1}{Re\left(\frac{\partial}{\partial y^*}\left(\frac{\partial v^*}{\partial y^*}\right)+\frac{\partial}{\partial x^*}\left(\frac{\partial u^*}{\partial x^*}\right)\right)\frac{\partial P^*}{\partial y^*}} \quad (26)$$

$$\frac{\partial \theta}{\partial t^*}+\frac{\partial (u^*.\theta)}{\partial x^*}+\frac{\partial (v^*.\theta)}{\partial y^*}=\frac{1}{Re.Pr\left(\left(\frac{\partial \theta}{\partial x^*}\right)^2+\left(\frac{\partial \theta}{\partial y^*}\right)^2\right)}-\frac{Br}{Re.Pr\left(2\left(\left(\frac{\partial u^*}{\partial x^*}\right)^2+\left(\frac{\partial v^*}{\partial y^*}\right)^2\right)+\left(\frac{\partial u^*}{\partial y^*}+\frac{\partial v^*}{\partial x^*}\right)^2\right)} \quad (27)$$

6. Dimensionless initial and boundary conditions

Given that 0≤ x ≤ℓ and 0≤ y ≤2R, based on Eqs. (9) and (10), the variables are bounded between zero and one after non-dimensionalization. On the other hand, based on Eqs. (12), (13), (14) and (19) the dimensionless initial and boundary conditions can be written as follows:

$$x^*=0 \quad \begin{cases} u^*=1 \\ v^*=0 \\ \theta=1 \\ P^*=1 \end{cases} \quad \text{and} \quad \begin{cases} y^*=0 \\ y^*=1 \end{cases} \quad \begin{cases} u^*=0 \\ v^*=0 \\ \theta=0 \end{cases} \quad (28)$$

7. Computational fluid dynamics (CFD) technique to solve the numerical model

The resulting dimensionless equations are relatively long and practically unsolvable. Drawing on CFD techniques, the distributions of dimensionless velocity, dimensionless pressure and dimensionless temperature in the flow of the two reference crude oils can be calculated and analyzed at various points along the pipe.

The finite volume method is a standard CFD technique that is employed in the beginning to discretize the computational domain (solution field) and create a computational grid. Next, the general form of the dimensionless governing equations is considered. By integrating the general equation and discretizing its terms, a suitable algorithm is obtained for discretizing the dimensionless equations governing the problem in the computational grid. Another step in the CFD technique is to solve the system of algebraic equations obtained by discretizing the equations, which is carried out by the iterative Tri-Diagonal Matrix Algorithm (TDMA) method due to complexity. Accordingly, the velocity and pressure of the Power-law crude oil flow are calculated for all Control Volumes (CVs) throughout the grid using dimensionless continuity and momentum equations. On the other hand, the flow velocity and pressure are coupled in dimensionless equations. Therefore, before taking the TDMA approach, the Semi-Implicit Method for Pressure-Linked (SIMPLE) algorithm [22] is used to obtain the correct correlation between flow velocity and pressure (pressure–velocity coupling algorithm).

Calculating the dimensionless temperature for each of the reference crude oils using the dimensionless energy equation is contingent upon knowing the dimensionless velocity in any CV of fluid. By substituting the estimated dimensionless velocity in the equation, the dimensionless temperature of the fluid is also determined in any CV of the computational grid.

8. Input data

To avoid calculation complexities and duplicate explanations in the numerical methods ahead, the simplified forms of the dimensionless variables are introduced to dimensionless equations and the dimensionless initial and boundary conditions, for example $x^* \to x$. Under steady state, Eqs. (24) through (27) can be written as follows:

$$\frac{\partial u}{\partial x}+\frac{\partial v}{\partial y}=0 \quad (29)$$

$$\frac{\partial u^2}{\partial x}+\frac{\partial (u.v)}{\partial y}=\frac{1}{Re\left(\frac{\partial}{\partial x}\left(\frac{\partial u}{\partial x}\right)+\frac{\partial}{\partial y}\left(\frac{\partial v}{\partial y}\right)\right)\frac{\partial P}{\partial x}} \quad (30)$$

$$\frac{\partial v^2}{\partial y}+\frac{\partial (v.u)}{\partial x}=\frac{1}{Re\left(\frac{\partial}{\partial y}\left(\frac{\partial v}{\partial y}\right)+\frac{\partial}{\partial x}\left(\frac{\partial u}{\partial x}\right)\right)\frac{\partial P}{\partial y}} \quad (31)$$

$$\frac{\partial (u.\theta)}{\partial x}+\frac{\partial (v..\theta)}{\partial y}=\frac{1}{Re.Pr\left(\left(\frac{\partial \theta}{\partial x}\right)^2+\left(\frac{\partial \theta}{\partial y}\right)^2\right)}\frac{Br}{Re.Pr\left(2\left(\left(\frac{\partial u}{\partial x}\right)^2+\left(\frac{\partial v}{\partial y}\right)^2\right)+\left(\frac{\partial u}{\partial y}+\frac{\partial v}{\partial x}\right)^2\right)} \quad (32)$$

Moreover, the dimensionless initial and boundary conditions can be written:

$$x = 0 \quad \begin{cases} u = 1 \\ v = 0 \\ \theta = 1 \\ P = 1 \end{cases} \quad \text{and} \quad \begin{cases} y = 0 \\ y = 1 \end{cases} \quad \begin{cases} u = 0 \\ v = 0 \\ \theta = 0 \end{cases} \tag{33}$$

Next, to solve the above equations and obtain the dimensionless velocity, pressure and temperature for each reference crude oil in the computational grid by CFD technique, it is necessary to estimate Re, Pr and Br along the pipe by Eqs. (6) through (8) for each fluid. Accordingly, taking into account the pipe specifications including 2R=21 cm and ℓ=300 cm the input data mentioned in Table 5, are required. It must be noted that the last term on the right side of Eq. (32) will be 0 due to the lack of heat dissipation on the centerline, where Br is 0 [15].

Table 5. Input data

Reference crude	Density (ρ) (g/cm³)	Viscosity (μ) (Pa.s)	Entry velocity (v_{in}) (cm/s)	Temperature (T_w) (°C)	Specific heat capacity (K) (W/m °C)	Thermal conductivity (C_P) (J/g °C)	Calculated	
							Re	Pr
A	0.87	0.09	10	22	0.13	1.83	2019	1.27
B	0.89	0.20	10	22	0.14	1.90	649	3.93

Because of the heat dissipation, Br is not 0 in the area between the interior surface and the centerline. Given the above input data and Eq. (19), Br appears in the last term on the right side of Eq. (32) based on the relations below:

Br= -0.71/4θ for the reference crude oil A (34)

Br= -2.07/4θ for the reference crude oil B (35)

Under the dimensionless initial and boundary conditions, CFD calculations for each reference crude oil are based on Eqs. (29) through (32).

9. Convergence and the rate of solution

A numerical solution has been developed in an attempt to determine the distribution of velocity, pressure, and temperature of the reference crude oil on a non-collocated computational grid by CFD technique according to the preceding chapter where an under-relaxation factor is used to prevent the solution divergence. Applying the under-relaxation factor affects the convergence and rate of the solution. Lowering the factor down to 0.05 does not have a significant impact on the convergence and only reduces the rate of the solution. By increasing the factor, it is unlikely that the discussed parameters (velocity, pressure, and temperature) can be optimized but it should be noted that with this increase, the solution does not tend to diverge. The under-relaxation factor is assumed at 0.15. In addition to the under-relaxation factor, the number of CVs must also be optimized to prevent considerable computational error on the one hand and high computational costs on the other. It must be noted that a sub-optimal number of CVs exacerbates the error, whereas too many of them result in excessive computational costs.

9.1. Velocity Distribution over the Centerline and the Optimal Number of CVs

To determine the optimal number of CVs, first the computational domain is discretized into an assumed number of CVs, then, it suffices to calculate the velocity of reference crude oil B on the centerline (Table 6). As shown in Table 6, the velocity distribution does not change significantly on the centerline by increasing CVs above a certain number.

It must be noted that flow variables are dimensionless. Therefore, the dimensionless velocity at the start of the centerline (the pipe inlet) is known and equal to 1.

Table 6. Number of CVs in calculations

Reference crude oil B	Number of CV			
	44x44	55x55	66x66	77x77
U_{max} on centerline	1.46	1.37	1.29	1.33

As Figure 3 shows, the curves gradually unite as the number of CVs is increased. Also, reaching the end of the centerline and from (about) $x = 0.95$ to the next, the fluid velocity reaches its maximum value based on each of the number of CVs assumed. Moreover, Table 6 shows the maximum velocity of the reference crude oil B on the centerline for different numbers of CVs. Increasing the CVs above 66×66 does not result in a considerable improvement. Therefore, to achieve higher calculation accuracy, the highest number of CVs (77×77) is taken as optimal.

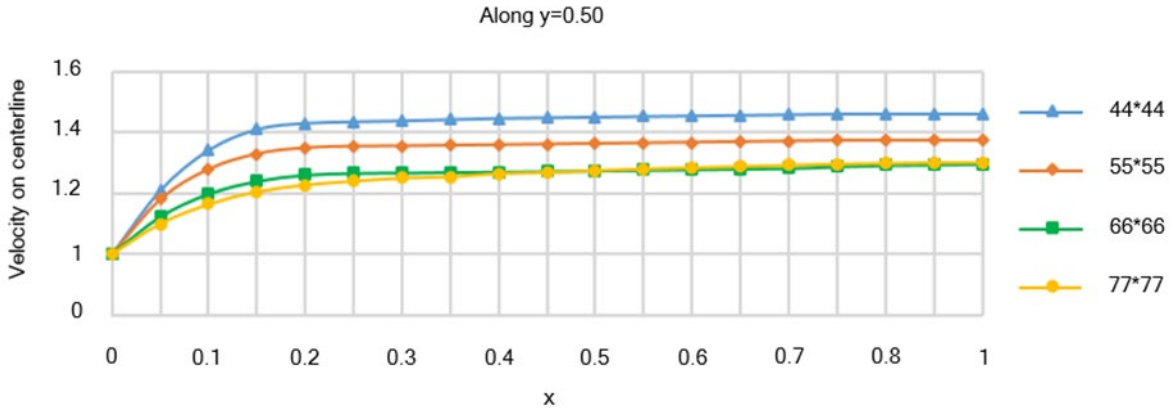

Figure 3. Velocity distribution of reference crude oil B on centerline from start to pipe end against number of CVs

10. Results and discussion

The validity of the proposed model including the validity of all assumptions, input parameters, numerical methods, and the computer code written in MATLAB is determined by comparing numerical results of this study with those in the literature under the same governing conditions. Accordingly, while confirming the accuracy of numerical results, it will be shown that the proposed model benefits from the simultaneous capabilities of several models.

The number of studies compared is limited considering structural equations, flow path, flow mechanism, flow behavior index, shear rate range and initial and boundary conditions. To examine the validity of the numerical model in this study, the results are compared with those obtained from the other studies [14-15,19] for the same systems.

To ensure the performance of the numerical model, the fully developed flow of the reference crude oils A and B is, respectively, studied with the flow behavior index 0.99 and 0.5.

As previously mentioned, the heat dissipation in the energy equation affects the temperature distribution of a Power-law fluid flowing in a pipe. The heat dissipation on the centerline is 0 and can thus be ignored (Br=0). In this case, the last term can be deleted from the right-hand side of the energy equation and its dimensionless form. The dimensionless numerical results of this study are compared with those in these three studies.

10.1. Velocity of power-law crude oil

As shown in Table 7, the numerical results of the present study on each of the reference crude oils samples at the cross-section of x=0.95 on the centerline, are compared with those obtained from Skelland's study on the maximum dimensionless velocity of a Power-law fluid on the centerline [14]. Table 7 indicates the nearly identical results of both studies with maximum precision of ± 0.03. It can be claimed that the region $x \geq 0.95$ is located in the fully-developed region of fluid flow.

Table 7. Comparison of maximum dimensionless velocities of reference crude oils A and B on centerline between present study and those obtained from Skelland's study [14]

Reference crude oil	Present study	Skelland [14]
A	1.48	1.5
B	1.33	1.3

10.2. Temperature of Power-law Crude Oil

In the study of heat transfer in a fully developed flow of a Power-law fluid, by ignoring heat dissipation, a relation can be made between thermal conductivity, specific heat capacity, and fluid velocity at each point (x, r) [15].

$$C_P u \frac{\partial T}{\partial x} = K \frac{\partial^2 T}{\partial x^2} + \frac{K}{r}\frac{\partial}{\partial r}\left(r \frac{\partial T}{\partial r}\right) \quad (36)$$

Using Eq. (19) and dimensionless temperature, Eq. (36) can be rewritten as follows, which can be solved by separation of variables for given values in the range of 0≤n≤1 [23].

$$u \frac{\partial \theta}{\partial x} = \frac{K}{r C_P}\frac{\partial}{\partial r}\left(r \frac{\partial \theta}{\partial r}\right) \quad (37)$$

Given the numerical results of the present study, the purpose is to compare the results of two studies at the cross-section x=0.95. Since in the Chhabra and Richardson's study [15], the heat dissipation is ignored, so under the comparison conditions, the CVs of the computational grid is limited to the centerline. Table 8 compares the dimensionless temperatures calculated by the present study with those obtained from the Chhabra and Richardson's study [15]. Table 8 indicates the nearly identical results of both studies with maximum precision of $+0.04$.Therefore, it can be claimed that the region $x \geq 0.95$ is located in the fully-developed region of fluid flow.

Table 8. Comparison of dimensionless temperatures of reference crude oils A and B on centerline between present study and those obtained from Chhabra and Richardson's study [15]

Reference crude oil	Present study	Chhabra and Richardson's [15]
A	0.27	0.24
B	0.66	0.62

10.3. Pressure drop in flow of power-law crude Oil

Since in the present study the two-dimensional flow of power-low crude oils is considered, so the numerical results can be compared with those obtained from Etemad *et al.*'s study for the same system [19]. Etemad *et al.*'s study focused on a certain range of the flow behavior index, within which the index 0.99 is not included. Therefore, in this section, the comparison of the results of both studies is limited to the reference crude oil B with Re=649. Table 9 compares the dimensionless pressure drop of reference crude oil B in the vicinity of the wall/plate inner surface (y=0.05) obtained in this study with those obtained from Etemad *et al.*'s study in horizontal mode [19]. Table 9 indicates the nearly identical results of both studies with maximum precision of ± 0.05.

As shown in Tables 7-9, the nearly identical results indicate that the proposed numerical model in the present study has the simultaneous capabilities of the models proposed in all three studies of Skelland, Chhabra and Richardson, and Etemad *et al.* [14-15,19].

Table 9. Comparison of dimensionless pressure drop of reference crude oil B in vicinity of wall / plate inner surface between present study with those obtained in Etemad *et al.*'s study

	x					
	0.05	0.25	0.5	0.7	0.8	0.9
Present study	0.26	0.27	0.07	0.03	0.01	0.01
Etemad *et al.* [19]	0.24	0.22	0.09	0.05	0.03	0.02

11. Conclusions

A numerical model based on the rheological behaviors of reference crude oils samples, the relation between mass transfer and heat transfer and by taking into account heat dissipation, is presented for calculating the velocity, pressure and temperature distributions along a pipe.

This numerical model has the simultaneous capabilities of the models reported in previous studies by Skelland, Chhabra and Richardson, and Etemad *et al.* [14-15,19]. In this regard, the most important conclusions can be summarized as follows:

The number of CVs has been optimized to prevent considerable computational error on one hand and high computational costs on the other. To determine the optimal number of CVs,

the maximum dimensionless velocity of reference crude oil B on the centerline of pipe is calculated based on the given number of CVs (44×44, 55×55, 66×66 and 77×77). As the number of CVs increases, the maximum dimensionless velocity of reference crude oil B on the centerline gradually tends to unity for different numbers of CVs. The increase in the number of CVs above 66×66 does not result in a considerable improvement. Therefore, the highest number of CVs (77×77) is taken as optimal.

The optimal number of CVs (77×77) is used to discretize the computational domain, accordingly by applying a CFD technique, the desired numerical model is solved and the dimensionless velocity, pressure, and temperature of each reference crude oil are calculated. If the CVs number of 44×44 is considered to discretize the computational domain, then the dimensionless velocity of reference crude oil B will be 1.46. This result, in comparison with the dimensionless velocity obtained from the Skelland's study [14] for the same system, is faced with the precision of +0.16. Applying the CVs number of 44×44 results in increasing the error of result compared to conditions where the CVs number of 77×77 (with the precision of +0.03) is applied.

Considering the CVs number of 44×44 to discretize the computational domain, the dimensionless pressure drop of reference crude oil B in the vicinity of the pipe wall and at the points x=0.05, 0.5 and 0.9 are, respectively, 0.19, 0.06 and 0.01. These results, in comparison with the dimensionless pressure drop obtained from the Etemad *et al.*'s study for the same system [19], are, respectively, faced with the precision of -0.05, -0.03 and -0.01. Applying the CVs number of 44×44 results in increasing the error of result compared to conditions where the CVs number of 77×77 (with the precision of +0.02, -0.02 and -0.01) is applied. Considering the CVs number of 44×44, the dimensionless temperatures of reference crude oils A and B on the centerline of the pipe are, respectively, 0.19 and 0.58. These results, in comparison with the dimensionless temperature obtained from the Chhabra and Richardson's study for the same system [15], are faced with the precision of -0.05, and -0.04. Applying the CVs number of 44×44 results in increasing the error of result compared to conditions where the CVs number of 77×77 (with the precision of +0.03 and +0.04) is applied.

For the reference crude oils A and B, near the inner surface, at the pipe inlet (the flow is developing) and at the pipe end (the flow is fully developed) the dimensionless velocity approaches 0 but increases on the centerline (y=0.50).

In the vicinity of the pipe wall, the velocity gradient of the crude oil sample B is sharper than that of sample A in this region. Further away from the pipe wall, the velocity gradients of both reference crude oils samples A and B decline until vanished. In fact, in comparison with the reference crude oil sample A, the flow of sample B reaches its maximum velocity at a closer distance from the pipe wall.

The reference crude oil sample A features a higher maximum velocity than sample B in the inlet region. In other words, at this cross-section, the closer the behavior index of the paraffinic crude oil to 0.50, the lower the maximum velocity of the flow. Since Reynolds number is a function of the flow behavior index, therefore in the pipe inlet region, the flow of reference oil with higher Reynolds number has lower velocity.

The reference crude oil sample A features a higher maximum velocity than sample B at the pipe end. In other words, at the pipe end, the flow of reference crude oil with higher Reynolds number has lower velocity.

The decline in the flow velocity in spite of the steeper velocity gradient near the inner surface of the pipe as a result of heat transfer to the pipe wall and the higher flow velocity further toward the centerline where velocity is at maximum. Put differently, the lower velocity of the flow near the pipe wall is indicative of a pressure drop in the region.

The reference crude oil sample B features a more substantial pressure drop than sample A along the pipe and in the vicinity of its wall. In other words, near the inner surface of the pipe, the flow of the reference crude oil with lower Reynolds number and higher Prandtl number has a higher-pressure drop.

Near the inner surface of the pipe, the pressure drop is more considerable with the reference crude oil sample B due to its higher viscosity than the sample A. Put differently; the

higher viscosity of the crude oil sample B increases its resistance against the exerted stresses, as well as the pressure drop across the flow.

In the inlet region, the dimensionless temperatures of reference crude oils samples B and A approach a developed state. In this region, the stresses exerted on the fluid begin to disappear with the temperature gradient vanishing.

Comparison of the dimensionless temperatures of reference crude oils B and A in the pipe inlet region, between the pipe wall and centerline indicates that in the y≤0.06 region, the flow of reference crude oil with lower Reynolds number and higher Prandtl number is faced with the lower temperature drop.

Comparison of the dimensionless temperatures of reference crude oils B and A near the pipe end, between the wall and centerline indicates that in the y≤0.05 region, the flow of reference crude oil with lower Reynolds number and higher Prandtl number is faced with the lower temperature drop.

List of variables

Brinkman number	Br
Specific heat capacity	c_P
Fluid specific heat capacity at pipe inlet	$c_{P_{in}}$
Dimensionless specific heat capacity	c_P^*
Gravitational acceleration on Earth in x direction	g_x
Gravitational acceleration on Earth in y direction	g_y
Consistency index of fluid	k
Thermal conductivity	K
Fluid thermal conductivity at pipe inlet	K_{in}
Dimensionless thermal conductivity	K^*
Pipe length	ℓ
Flow behaviour index	n
Fluid pressure	P
Fluid pressure at pipe inlet	P_{in}
Prandtl number	Pr
Dimensionless fluid pressure	P^*
Pipe radius	R
Reynolds number	Re
Radial distance from centerline	r
Fluid temperature	T
Fluid temperature at pipe inlet	T_{in}
Pipe wall temperature	T_w
Time	t
Fluid velocity in x direction	u
Maximum velocity in x direction	u_{max}
Slip velocity on pipe walls in x direction	u_{slip}
Dimensionless fluid velocity in x direction	u^*
Fluid velocity in y direction	v
Fluid velocity at pipe inlet	v_{in}
Slip velocity on pipe walls in y direction	v_{slip}
Dimensionless fluid velocity in y direction	v^*
Distance on longitudinal axis (horizontal)	x
Dimensionless distance on longitudinal axis (horizontal)	x^*
Distance on transverse axis (vertical)	y
Dimensionless distance on transverse axis (vertical)	y^*

Greek symbols

Dimensionless temperature	θ
Apparent viscosity	μ
Fluid viscosity at pipe inlet	μ_{in}
Dimensionless apparent viscosity	μ^*
Density	ρ
Fluid density at pipe inlet	ρ_{in}
Dimensionless density	ρ^*

Data availability

The data that support the findings of this study are available from the corresponding author upon reasonable request.

References

[1] Beggs, HD, and Robinson JR. 1975, Estimating Viscosity of Crude Oil Systems. Journal of Petroleum Technology, 1140-1141.

[2] Ely JF, and Hanley JM. 1981, Prediction of Transport Properties. Viscosity of Fluids and Mixtures. Industrial & Engineering Chemistry Fundamentals, 1981; 20: 323-332.

[3] Johnso, SE, Svrcek WY, Mehrotra AK. Viscosity Prediction of Athabasca Bitumen using Extended Principle of Corresponding States. Ind. Eng. Chem. Res,1987; 26: 2290.

[4] Agarwal KM, Purohit RC, Surianarayanan M, Josh, GC, and Krishna R. Influence of Waxes on Flow Properties of Bombay High Crude. Fuel,1989; 68:937-939.

[5] Lorge O, Djabourov M, and Brucy F. Crystallisation and Gelation of Paraffinic Crude Oils under Flowing Conditions. Oil & Gas Science and Technology, 1997; 52(2): 235-239.

[6] El-Gamal IM, Gad EAM. Low Temperature Rheological Behavior of Umbarka Paraffin Crude and Influence of Flow Improver. Colloids and Surfaces A: Physicochemical and Engineering Aspects, 1998; 131(1–3): 181-191.

[7] Chandaa D, Sarmaha A, Borthakura RA, Raoa KV, Subrahmanyama B, and Das HC. Combined Effect of Asphaltenes and Flow Improvers on Rheological Behavior of Indian Paraffinic Crude Oil. Fuel, 1998; 77 (11): 1163-1167.

[8] Kirsanov EA, Remizov SV. Application of Casson Model to Paraffinic Crude Oil. Rheol Acta, 1999; 38: 172.

[9] Alboudwarej H, Kempton E, and Huo Z. Flow-Assurance Aspects of Subsea Systems Design for Production of Paraffinic Crude Oils . SPE Annual Technical Conference 2006, San Antonio, Texas, U.S.A.

[10] Wardhaugh LT, and Boger DV. Flow Characteristics of Paraffinic Crude Oils: Application to Pipeline Design. AIChE J., 1991; 37 (6):871-885.

[11] Chang PY, Chou FC, Tung CW. Heat Transfer Mechanism for Non-Newtonian Fluid 2:1 Rectangular Duct. Int. J. Heat Transfer, 1998; 41: 3841-3856.

[12] Kané M, Djabourov M, and Volle JL. 2004, Rheology and Structure of Paraffinic Crude Oils in Quiescent and under Shearing Conditions. Fuel, 2004; 83(11,12): 1591-1605.

[13] Hamilton RL, and Crosser K. Thermal Conductivity of Heterogeneous Two- Component Systems. Industrial & Engineering Chemistry Fundamentals, 1962; 1:187-191.

[14] Skelland AHP. Non-Newtonian Flow and Heat Transfer. Wiley 1967, New York, USA.

[15] Chhabra RP, and Richardson JF. Non-Newtonian Flow and Applied Rheology. R.P.C.F. Richardson, Editor., Butterworth-Heinemann: Oxford 2008,1-55.

[16] Lightfoot EN. and Stewart WE. Transport Phenomena. Wiley 2007, New York, USA.

[17] Ryan NW, and Johnson MM. 1959, Transition from Laminar to Turbulent Flow in Pipes. AIChE J., 1959; 5 : 433.

[18] Mishra P, and Tripathi G. 1971, Transition from Laminar to Turbulent Flow of Purely Viscous Non-Newtonian Fluids in Tubes. Chem. Eng. Sci., 1971; 26:915-921.

[19] Etemad SGh, Mujumadar AS, and Huang B. Effects of Variable Viscosity and Viscous Dissipation on Laminar Convection Heat Transfer of a Power Law Fluid. Int. J. Heat Mass Transfer, 1994; 38 (2): 2225-2238.

[20] Mohammadi A, Mkhize M, Mohammadi AH. An Insight into Waxy Crude Oils Flow Curves Using Shear-Rotary Rheo-Metric Experiments and Power-law Model. Petroleum and Coal, 2019; 61(6):1330-1336.

[21] Mohammadi A, Mkhize M, Mohammadi AH. Experimental Analyses of Viscosity, Thermal Conductivity and Specific Heat Capacity of Waxy Crude Oil and a Computational Fluid Dynamics (CFD) Study. Petroleum and Coal, 2021; 63(2):366-372.

[22] Patankar SV. Numerical Heat Transfer and Fluid Flow. Taylor & Francis 1980, 1-39.

[23] Bird RB, Armstrong RC, and Hassager O. Dynamics of Polymeric Liquids. Fluid Dynamics, 1 (2), Wiley 1987, New York, USA.

To whom correspondence should be addressed: professor Dr. Amir H. Mohammadi, Discipline of Chemical Engineering, School of Engineering, University of KwaZulu-Natal, Howard College Campus, King George V Avenue, Durban 4041, South Africa, E-mail: amir_h_mohammadi@yahoo.com